**J. Cent. South Univ.** (2013) 20: 3282−3295
**DOI:** 10.1007/s11771-013-1852-9

Springer

# Vacuum preloading combined electroosmotic strengthening of ultra-soft soil

PENG Jie(彭劼)[1, 2], XIONG Xiong(熊雄)[1, 2], MAHFOUZ A H[3], SONG En-run(宋恩润)[1, 2]

1. Key Laboratory for Geomechanics and Embankment Engineering of Ministry of Education (Hohai University), Nanjing 210098, China;
2. Geotechnical Research Institute, Hohai University, Nanjing 210098, China;
3. Department of Civil Engineering, Faculty of Engineering, Jazan University, Jazan 45142, Saudi Arabia

© Central South University Press and Springer-Verlag Berlin Heidelberg 2013

**Abstract:** To assess the effectiveness of vacuum preloading combined electroosmotic strengthening of ultra-soft soil and study the mechanism of the process, a comprehensive experimental investigation was performed. A laboratory test cell was designed and applied to evaluate the vacuum preloading combined electroosmosis. Several factors were taken into consideration, including the directions of the electroosmotic current and water induced by vacuum preloading and the replenishment of groundwater from the surrounding area. The results indicate that electroosmosis together with vacuum preloading improve the soil strength greatly, with an increase of approximately 60%, and reduce the water content of the soil on the basis of consolidation of vacuum preloading, however, further settlement is not obvious with only 1.7 mm. The reinforcement effect of vacuum preloading combined electroosmosis is better than that of electroosmosis after vacuum preloading. Elemental analysis using X-ray fluorescence proves that the soil strengthening during electroosmotic period in this work is mainly caused by electroosmosis-induced electrochemical reactions, the concentrations of $Al_2O_3$ in the VPCEO region increase by 2.2%, 1.5%, and 0.9% at the anode, the midpoint between the electrodes, and the cathode, respectively.

**Key words:** vacuum preloading; electroosmosis; laboratory test; ultra-soft soil; reinforcement effect; X-ray fluorescence; reinforcement mechanism

## 1 Introduction

The rapid reinforcement and treatment of ultra-soft soil is an important issue in geotechnical engineering. The demand for land is increasing due to global economic development; however, the scarcity of land resources is also increasing. Therefore, land reclamation near coastlines has been adopted to compensate for the deficiency of land resources. In China, for example, more than 300 $km^2$ of new land has been reclaimed from the sea annually in recent years [1]. Silt mixed with muddy water which is the major component of the coastal seabed is deposited to form liquid to liquid-plastic state ultra-soft soil. As a result, the bearing capacity of the ground formed for reclamation is not sufficient to meet the engineering needs for further development.

The principles of vacuum preloading were firstly introduced by KJELLMAN [2]. This method involves several key steps. First, after the insertion of prefabricated vertical drain (PVD), the reinforcement area is sealed with a membrane. Second, the pressures below the sealing membrane and within the PVD decrease with vacuum pumping. Due to the poor permeability of the soil, the decrease in pore pressure of the soil is slower than the pressure decrease in the PVD, and the pressure difference is developed between the soil and the PVD. The pore water is drived from soil to the PVD by the pressure difference, which leads to a decrease in pore pressure of the soil with the total stress unaltered. As a result, the effective stress of the soil increases to accelerate consolidation. After the proposition of the principle, many scholars have studied the consolidation mechanism, calculation methods and construction technologies of vacuum preloading [3−4], and the method has been widely used in the world. The low construction loads of the vacuum preloading (VP) method enable construction on sites with a very low bearing capacity; therefore, this method has been increasingly applied to the reinforcement engineering of ultra-soft soil and reclamation silt sites [5]. However, due to the limitation of atmospheric pressures, the designed vacuum load is generally no lower than −80 kPa;

**Foundation item:** Project(2009B13014) supported by the Fundamental Research Funds for the Central Universities of China; Project(IRT1125) supported by the Program for Changjiang Scholars and Innovative Research Team in University, China
**Received date:** 2012−06−15; **Accepted date:** 2012−09−20
**Corresponding author:** PENG Jie, Associate Professor; Tel: +86−25−83787918; E-mail: peng-jie@hhu.edu.cn

therefore, the reinforcing effect of this method is subjected to certain restrictions. This effect can be improved by combining VP with other methods, such as the vacuum combined surcharge preloading, which involves surcharge preloading and vacuuming at the same time, resulting in an improved reinforcing effect and a more stable foundation. This method has been applied to soft foundation treatments more widely [6−7], and in ultra-soft ground, a surcharge loading is difficult to apply. Thus, the electroosmosis combined with VP is recommended for projects requiring a high reinforcement of ultra-soft soil or reclamation silt because this method requires a comparatively smaller construction load.

The electroosmosis of porous material was first reported by REUSS in 1809 [8], and CASAGRANDE applied the electroosmosis in slope reinforcement works for the first time [8]. The electroosmosis involves the insertion of electrodes in the soil and the passage of a DC current through the soil. When the soil particles are in contact with water, two layers of ions of opposite charge and an equal amount of electrical charge, i.e., the electric double layer will form on the soil particle surface and near the liquid. The ions in the diffusion layer below the electric field migrate toward the opposing electrode, which cause the water molecules to move together such that the water drains; this phenomenon is known as electroosmosis. Through electroosmosis, the water content is reduced, and the strength of the soil is improved. In addition to the low construction loads of the electroosmosis, the drainage rate depends primarily on the electrical permeability of the soil instead of the soil hydraulic permeability. Therefore, this method is suitable for the reinforcement of silt, silty clay, and sludge with a low permeability coefficient. Extensive researches have been carried out on the effect of various types of soil on electroosmosis [9−10], the improvement of electroosmotic efficiency [11], and computational methods [12], and there are some successful electroosmosis trial tests in soft clay [13−14]. However, because of the shortcomings of the the electroosmosis, such as high power and electrode consumption, and escaping air bubbles in the process of electroosmosis, it has not yet been applied in a large scale.

The vacuum preloading can exhaust a portion of the free water out of the soil pores quickly and economicly, but its reinforcement effect is limited by atmospheric pressures. The electroosmosis is suitable for the reinforcement of soil with a low permeability coefficient, however, it is uneconomic to treat the soil with high water content due to the high power and electrode consumption. To improve the effectiveness and economic value of vacuum preloading and electroosmosis, these methods can be combined. This method, called vacuum preloading combined electroosmosis (VPCEO) herein, involves vacuum preloading (VP) to reinforce soft ground by draining a portion of the free water out of the pores of the soil during the early stages of consolidation. In the later stages, the effects of VP gradually lessen, and electroosmosis is conducted. While the vacuum is maintained, electroosmosis induces partially free and weakly bound water in the soil pores to discharge, thereby the reinforcement effect is further improved. In addition, the electroosmosis is conducted in the late stage, and part of the pore water has been discharged by vacuum preloading, only a small part of the pore water is discharged by electroosmosis; thus, the total costs will marginally increase. Therefore, the VPCEO method is potentially suitable for soft soil treatment.

The combined effects of VP and electroosmosis were firstly reported for dewatering of mineral slurries [15]. Subsequently, GAO et al [16] and FANG et al [16] conducted laboratory tests of the VPCEO consolidation method and studied the reinforcement effect when investigating alkaline residue soil. They observed that the combined effect improved the drainage rate and quantity and reduced the concentration of chloride ions. When the VP consolidation process was completed (i.e., no further drainage), the electroosmosis continued to produce a significant drainage effect [16]. The use of the VPCEO as a novel approach for the potential treatment of soft soils is currently in the early stages of research, and the implementation, reinforcement effect, reinforcement mechanism of this method remain uncertain, especially, whether the vacuum does improve the electroosmosis, and the difference between electroosmosis with or without vacuum preloading, have not been reported in the literature.

In this work, we first designed a laboratory test cell for VPCEO. Factors, such as the water flow direction caused by electroosmosis and VP and groundwater recharge in the process of VP, were taken into consideration. Two sets of comparative tests were conducted in parallel in the laboratory test cell. Test A involved VPCEO, electroosmosis was conducted when the VP drainage consolidation effect became weak, while a vacuum was maintained. The combined reinforcement process was allowed to continue for a specified duration before the conclusion of the test. Test B involved electroosmosis followed by VP, called electroosmosis after vacuum preloading (EOAVP) herein, the vacuum was stopped when the drainage and consolidation effect became weak, and electroosmosis was then conducted. Electroosmosis was allowed to continue for a specified duration before the conclusion of the test. During the tests, the soil deformation, pore pressure, water drainage, and power consumption were monitored and analyzed. After the tests, the soil strength and water content were measured. The reinforcing effects of the VP, VPCEO,

and EOAVP methods were investigated, and the difference between electroosmosis with or without VP were compared. Elemental analyses of the soil samples were conducted before and after the tests, and the reinforcement mechanism and applicability of VPCEO were discussed.

## 2 Laboratory tests

Currently, two types of systems are used for testing VPCEO, including a one-dimensional system (for the dehydration of tailings) (Fig. 1.) and a model cell system established by FANG et al [17] (Fig. 2). However, in practical soil treatment engineering, the conditions are largely different from those for a one-dimensional system.

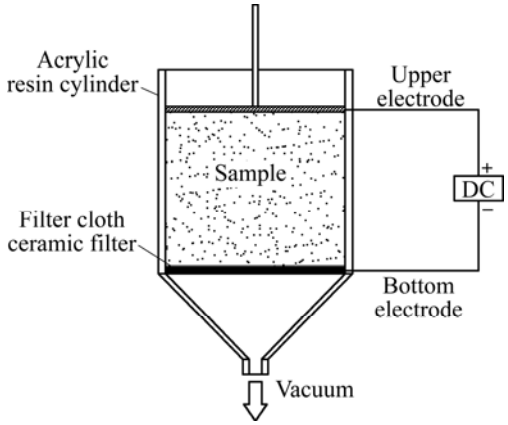


**Fig. 1** Schematic diagram of one-dimensional apparatus for electrokineticlly enhanced vacuum dewatering [15]

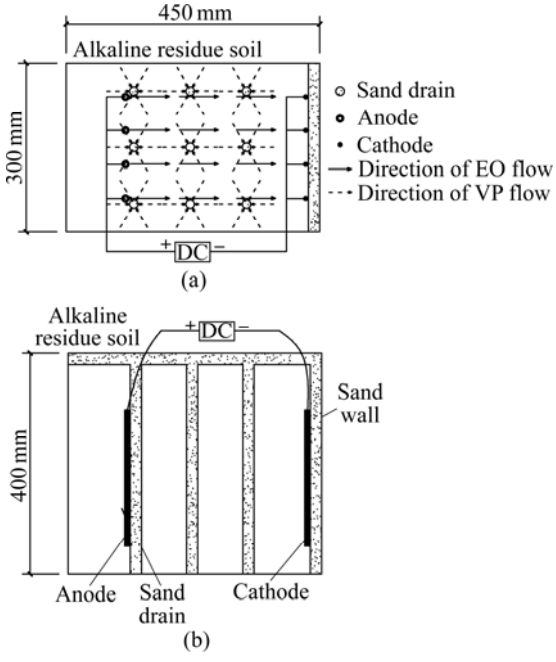


**Fig. 2** Schematic diagram of test cell for vacuum preloading combined electroosmosis: (a) Plan view; (b) Elevation view [17]

Regarding the model cell test by FANG et al [17], the direction of the electroosmotic flow and the flow of water induced by VP interfered with each other, as illustrated in Fig. 2. In addition, the replenishment of groundwater was not taken into consideration. In practice, during VP, the replenishment of water in the reinforcement area from periphery groundwater sources, which is driven by the reduction of the pore pressure and subsequent pore water loss in the reinforcement area soil, will significantly affect the soil seepage characteristics, mechanical properties, and water drainage volume, as well as the soil-strengthening effects.

Therefore, in the design of the laboratory test cell used in this work, a rational positioning of the electrode and PVD was considered to align the direction of the electroosmotic flow and water flow induced by VP, thereby allowing the two flows to work together, rather than interfering with each other. In addition, the water level surrounding the test cell was maintained above the surface of the reinforcement area to simulate the replenishment of water from periphery groundwater sources.

### 2.1 Test Apparatus

The test apparatus consisted of several components:

1) The test cell was constructed using transparent plexiglass with a thickness of 1 cm. The inner dimensions of the test cell were 1.0 m long, 1.0 m wide and 0.7 m high.

2) A single-stage rotary TW-4A vacuum pump with a power output of 0.37 kW was used. The pumping rate was 4 L/s with a vacuum pressure limit of 758 mmHg (100.8 kPa).

3) DC-powered electroosmosis was performed using a Zhaoxin RXN-605D regulated power supplied with a maximum voltage output of 60 V and a maximum current output of 5 A. The voltage and current could be adjusted within a fixed allowable range.

4) While the vacuum pump used in this work could not come into contact with water or moisture, a water&air separation bottle was employed to separate the water from the air that was extracted. Because the bottle was constructed using transparent plexiglass, the amount of liquid that was extracted could be readily recorded.

5) A vacuum control device was constructed by connecting a vacuum gauge to an on/off control box. The maximum reading of the vacuum gauge was 100 kPa with a sensitivity of up to 1 kPa. The vacuum gauge could be switched on and off automatically according to the vacuum present within the system. The combination of the vacuum gauge with the on/off controls allowed for precise control of the vacuum applied in the system to maintain the desired pressure.

6) The data acquisition devices included a TS3860

signal acquisition instrument, dial indicator, electronic scales, meters, and pore pressure probes.

The following materials were used in this work:

1) Electrodes: To facilitate the analysis of electroosmosis in the process of metal ion transport, aluminum was selected as the anode and copper was selected as the cathode. The cathode was fabricated using a copper tube with an outer diameter of 10 mm and an inner diameter of 8 mm. The anode was fabricated using a solid aluminum tube with a diameter of 10 mm. Both electrodes were 55 cm in length.

2) PVD: The dimension of the PVD was 4 mm × 20 mm, and it was cut from a SPB-II PVD with a vertical flow capacity of 8 $cm^3/s$.

3) Sealing membrane: The sealing membrane was constructed from a 0.14 mm thick PVC film. The longitudinal tensile strength was ≥18.5 MPa, the transverse tensile strength was ≥16.5 MPa, the maximum elongation was ≥220%, the right angle tear strength was ≥40 N/mm, and the permeability coefficient was $\geq 2.0\times10^{-10}$ cm/s.

The test apparatus was assembled according to Fig. 3(b). The prepared soil was placed inside the test cell, and PVDs were inserted at a depth of 60 cm to form a square layout with a spacing of 25 cm. The number of PVDs and their location are depicted in Fig. 3(a), and one of the actual test cells is presented in Fig. 4. The electrodes were then inserted into the soil according to the locations specified in Fig. 3. A layer of filter paper was wrapped around the copper cathode tube with an outer diameter of 10 mm and an inner diameter of 8 mm, facilitating the removal of water and gas induced by electroosmotic flow. The cathode was inserted in such a manner that the filter paper was always in contact with the drainage blanket under the membrane to ensure water discharge throughout the test. The anode, a solid aluminum

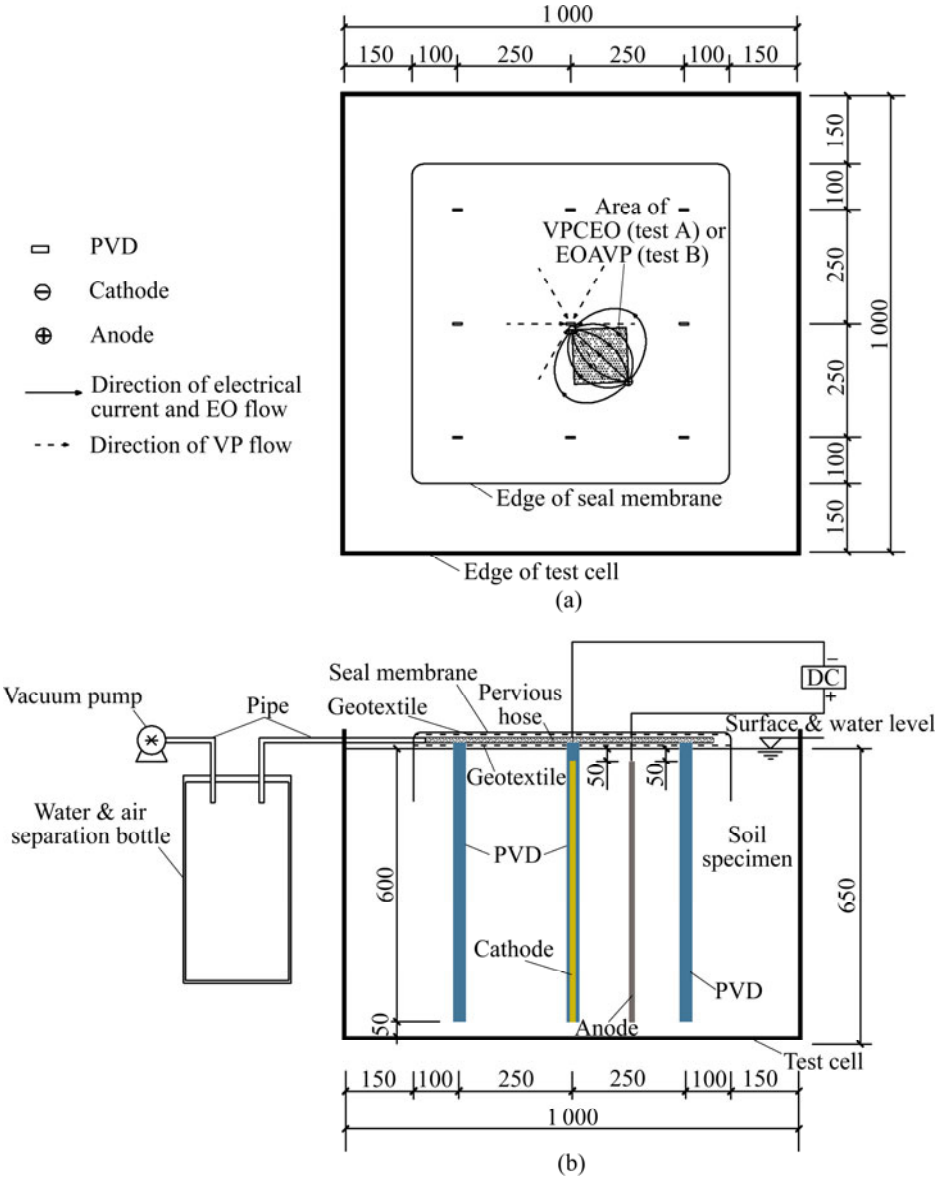


**Fig. 3** Schematic diagram of test cell (unit: mm): (a) Plan view; (b) Elevation view

**Fig. 4** Photo of test cell before reinforcement

rod of 10 mm in diameter was inserted into the soil, with the boundary condition of undrained. The anode was connected to the positive terminal of the power supply, and the cathode was connected to the negative terminal. Taking into consideration the settlement of the soil, an additional 5 cm soil layer was remained above the top of the electrodes to prevent damage to the sealing membrane. Before treatment, the bottoms of both electrodes and PVDs were adjusted to the same level in the soil. There was a 5 cm thick soil layer under the bottom of the PVDs and electrodes to be the means of sealing. The lengths of both the anode and cathode were 55 cm. The position of each electrode is illustrated in Fig. 3. The anode was placed in the center of a square constructed using four PVDs, whereas the cathode was placed adjacent to the middle PVD. This arrangement ensured that the current flow direction was aligned with the water flow induced by VP, as illustrated in Fig. 3(a).

A layer of non-woven geotextile (100 g/m$^2$) and a pervious hose were placed on the top of the soil. The hose was 2 cm in diameter and had tiny holes to transfer a vacuum. The exposed parts of the PVDs were connected to this hose, and the joint was wrapped with the non-woven geotextile to prevent it from being blocked by soil. An additional layer of geotextile was then placed on the top, followed by a sealing membrane. The edges of the sealing membrane were then buried in the soil at a position 15 cm from the test cell wall to simulate the field practice of real treatment systems. Taking into consideration the effect of replenishing groundwater during the VP process, water was continuously added to maintain the water level located in the surface of the soil sample. The pervious hose was connected to the vacuum pump outside of the sealing membrane so that the vacuum pressure could be transferred below the membrane.

### 2.2 Test soil preparation and its physical and mechanical properties

The test soil used in this work was acquired from the Dingshan reclamation site in Wenzhou City in Zhejiang Province, China. The site was formed by the deposition of hydraulic fill seabed mud along the coast of the Longwan District of Wenzhou. The collected soil was left to dry, broken, and passed through a 2 mm sifter. Deionized water was then added to form soil with a water content of 58.5%. Initially, the soil appeared to be liquid to liquid-plastic state, which was layered into the test cell and allowed to stand. The PVDs were then inserted, and after 15 d, the self-weighted consolidation was complete, and the average water content is 57%.

Particle analysis was conducted using a BT-9300H laser particle analyzer on four soil samples. The measured particle size gradation curve is plotted in Fig. 5. All particles within the soil were identified as clay with sizes less than 0.05 mm in diameter. The main geotechnical properties of the soil are listed in Table 1. The undrained shear strength was measured at depth of 25 cm using an E-286 vane shear apparatus, and the vane shear dimensions were 16 mm × 32 mm.

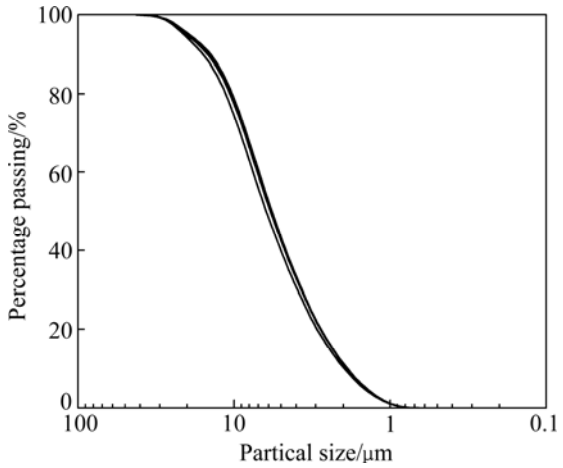


**Fig. 5** Grain size distribution curve of soil

### 2.3 Parallel comparison tests

Two sets of tests were conducted in parallel in the test cell (test A and test B). Vacuum pumping was conducted after all the measurement probes and related equipment were in place. During the testing process, the water level was maintained at the soil sample surface. Figure 6 shows a plot of the vacuum load throughout the entire test. The vacuum pressures of both tests A and B were basically maintained to be lower than −80 kPa.

In test A, electroosmosis was conducted after 25 d of vacuum loading when there was no drainage and settlement, with an applied voltage of 10 V. The combination of VP and electroosmosis was allowed to continue for 5 d.

In test B, after 25 d of vacuum loading when there

**Table 1** Geotechnical properties of original soil sample

| Property | Average value | Property | Average value |
|---|---|---|---|
| Specific gravity of soil, $G_s$ | 2.70 | Water content, $\omega$/% | 57.5% |
| Liquid limit, $\omega_L$/% | 54.6 | Void ratio, $e$ | 1.553 |
| Plastic limit, $\omega_P$/% | 33.1 | Compression index, $C_{cv}$ | 0.39 |
| Density, $\rho$/(g·cm$^{-3}$) | 1.67 | Permeability coefficient, $k$/(cm·s$^{-1}$) | $1.3\times10^{-6}$ |
| Undrained shear strength, $C_u$/kPa | 9.0 | Consolidation coefficient, $C_v$/(cm$^2$·s$^{-1}$) | $4.1\times10^{-4}$ |
| Pre-consolidation pressure, $p_c$/kPa | 27 | | |

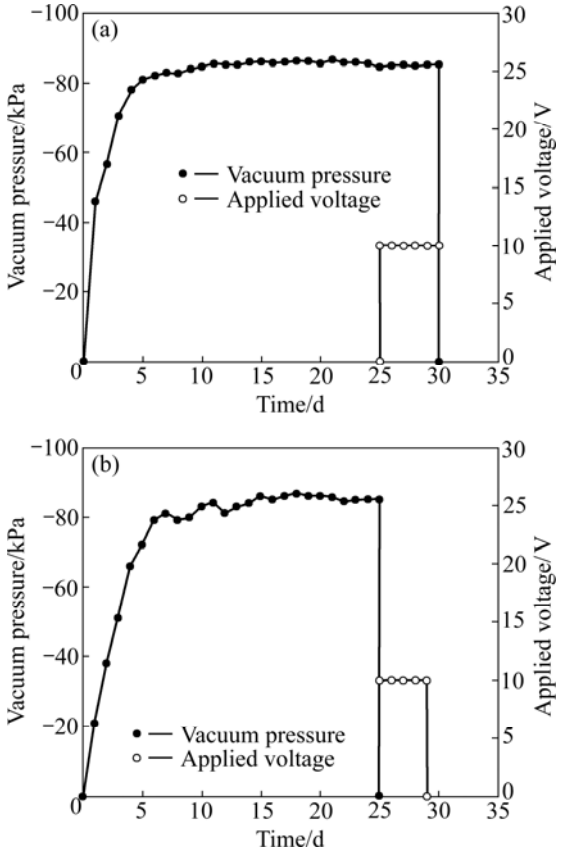


**Fig. 6** Variation with time of vacuum pressure under sealing membrane and applied voltage: (a) Test A; (b) Test B

was no drainage and settlement, the test cell was brought back to atmospheric pressure before the conduction of electroosmosis. The applied voltage was 10 V, and electroosmosis was allowed to continue for 4 d.

It is presented in Fig. 3(a) that the 2D-distribution of the current lines along the plane of the pair of electrodes during electroosmosis. The effective area under electroosmosis is shaded in Fig. 3(a) [18]. According to the arrangement of the electrodes and the effective electroosmotic regions, the test cell under the sealing membrane was divided into two sections. In test A, it could be divided into the pure VP region and the VPCEO region (the shade area in Fig. 3(a)); in test B, the test cell could be divided into a VP region and an EOAVP region (the shade area in Fig. 3(a)).

The pore pressure, settlement, water inflow and outflow, and electrical energy consumption were monitored in this work. The monitoring points for settlement and pore pressure are indicated in Fig. 7. For measurements of the pore pressure, two gauges with different depths (25 cm and 45 cm) were configured for each point. Monitoring of both the current and voltage was performed after the conduction of electroosmosis. After the tests, a vane shear test was conducted to measure the soil strength at different positions of the soil, and samples were collected to determine the water content and void ratio of the soil in the laboratory.

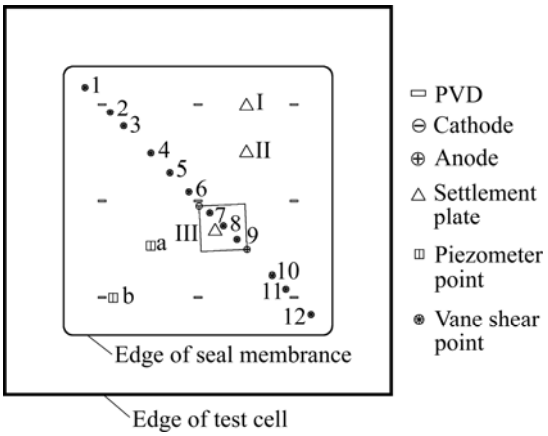


**Fig. 7** Location of monitoring and test points

## 3 Results

### 3.1 Settlement and lateral contraction

For comparative studies, three settlement measurement plates were placed on the sealing membranes in each test, as illustrated in Fig. 7. The settlement−time curves of tests A and B are plotted in Fig. 8. The final settlement values are summarized in Table 2.

Average settlements of 64.2 mm and 61.6 mm were observed during the VP phase for tests A and B, respectively. Settlement in the VPCEO region during electroosmosis in test A was observed to be 1.7 mm. Almost no settlement was detected in the VP region. For test B, the settlement was measured to be 1.2 mm in the EOAVP region during electroosmosis. In both tests A and B, soil settlement after electroosmosis was observed to

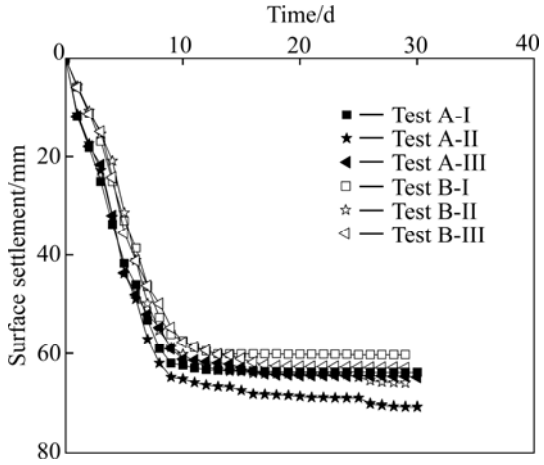


**Fig. 8** Surface settlement versus time

**Table 2** Summary of surface settlement

| Plate No. | Test A | | | Test B | | |
|---|---|---|---|---|---|---|
| | I | II | III | I | II | III |
| Settlement before electroosmosis/mm | 63.8 | 64.6 | 69.0 | 60.3 | 62.8 | 64.8 |
| Final settlement/mm | 63.9 | 64.8 | 70.7 | 60.3 | 63.0 | 66.0 |

be slight, accounting for 2.4% and 1.8% of the total settlement, respectively.

Lateral contraction of the soil occurred during the VP process in tests A and B, which ultimately led to the formation of crack between the test soil and cell wall, as depicted in Fig. 9. However, due to measurement limitations, the volume of cracks was not measured.

**Fig. 9** Crack between test soil and cell wall due to lateral contraction

### 3.2 Pore pressure

To monitor the variations in pore pressure, pressure gauges were positioned adjacent to the PVD (point b in Fig. 7) and in the middle of the four PVDs (point a in Fig. 7). The pressure gauges were buried at depths of 25 cm and 45 cm for each point.

The variations in pore pressure during the test are shown in Fig. 10. Due to the interference of the current in the soil during electroosmosis, the pore pressure data were only collected during VP, when a vibration wire gauge probe was used in the test.

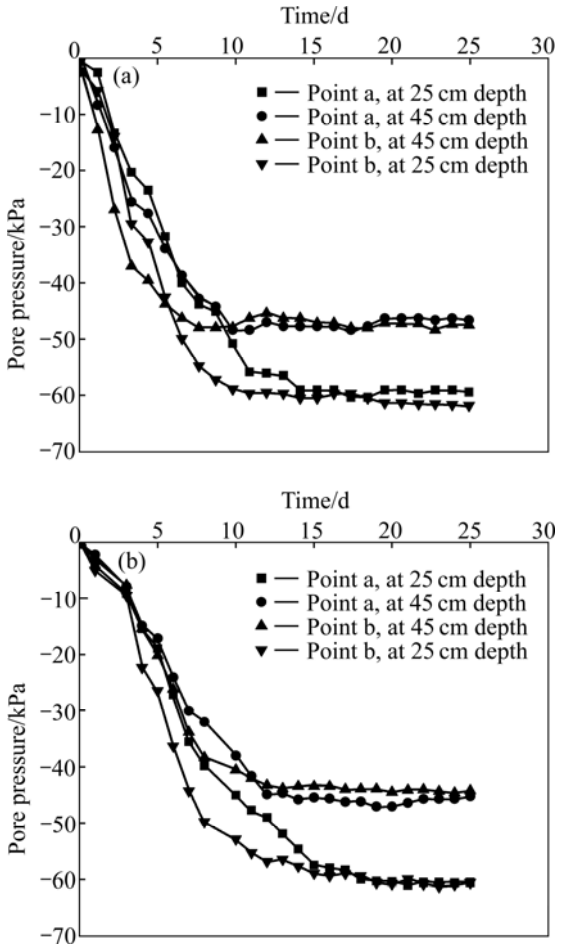


**Fig. 10** Measured pore pressure in soil: (a) Test A; (b) Test B

The pore pressure data collected in both tests A and B were similar. The reduction in pore pressure was observed to be greater at a shallow depth (25 cm depth). Furthermore, during the early stage of VP, the reduction in the pore pressure near the PVD was greater than that in the middle of the PVDs, but eventually converged to a similar level at the late stage of VP.

### 3.3 Drainage

Considering the effect of the groundwater around the reinforcement area in practical vacuum preloading engineering, water was supplemented during the test to maintain the water level above the soil sample surface.

Figure 11 reveals the net drainage during the test. From Fig. 11, it can be observed that the drainages for both tests A and B were relatively large during the early stages of VP. After 8−9 d, the drainage decreased significantly and was close to zero before electroosmosis. When electroosmosis was conducted, drainage increased slightly in test A, however, taking into account only 3.2% of the total reinforcement area of VPCEO area, the

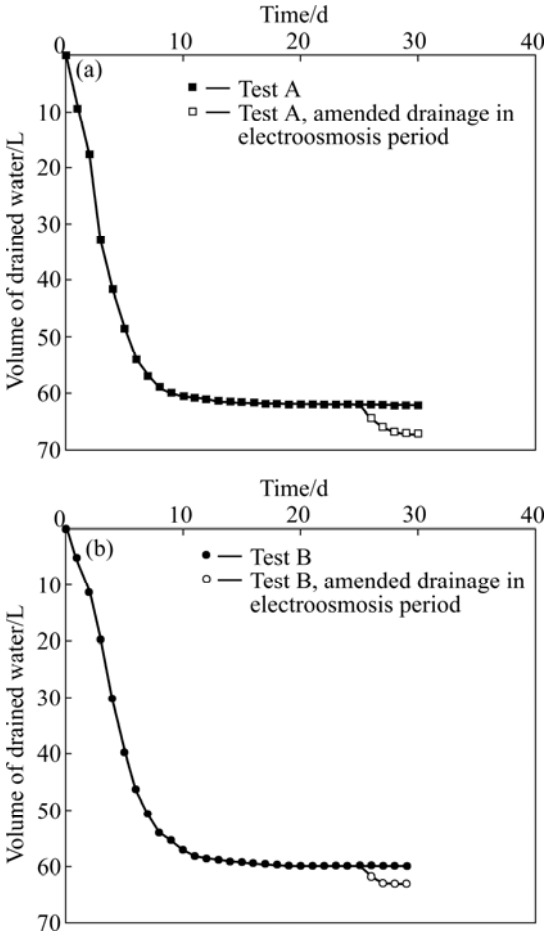


**Fig. 11** Variation of volumes of water drained with time: (a) Test A; (b) Test B

incremental drainage after electroosmosis was considerable. During the entire test, the net drainage of test A was 62.204 L, of which 62.045 L was discharged during VP. Thus, the net drainage during electroosmosis was 0.159 L. Considering the VPCEO area was 3.2% of the total reinforcement area, if all the reinforcement area was conducted with electroosmosis, the amended drainage during electroosmosis would be 4.983 L, accounting for 8.0% of the drainage during VP. Drainage occurring during the VP stage of test B is presented in Fig. 10(b), with a net drainage of 60.152 L, where 60.052 L was discharged during VP. Thus, the amended net drainage during electroosmosis was 3.143 L, accounting for 5.2% of the drainage during VP.

It shows from the drainage data that electroosmosis improved the drainage quantity when the VP consolidation process was completed, and the drainage of electroosmosis combined with VP was significantly greater than that of electroosmosis without VP.

### 3.4 Electrolysis at electrodes

During the process of electroosmosis in the tests, chemical reactions occur at both the anode and cathode. These reactions typically include the electrolysis of water and electrode redox reactions. The reactions at the anode are as follows:

$$M_A \longrightarrow M_A^{n+} + ne^- \quad (1)$$

$$2H_2O - 4e^- \longrightarrow O_2(\uparrow) + 4H^+ \quad (2)$$

The reactions at the cathode are as follows:

$$M_C^{n+} + ne^- \longrightarrow M_C \quad (3)$$

$$2H_2O + 2e^- \longrightarrow H_2(\uparrow) + 2OH^- \quad (4)$$

In these reaction schemes, $M_A$ and $M_C$ are metals used as the anode and cathode, respectively. As the chemical reaction proceeds, the anodic metal dissolves via oxidation, releases oxygen gas, and generates hydrogen ions. Metal precipitates at the cathode through reduction, thereby generating hydrogen gas and hydroxide ions. Both the hydrogen and hydroxide ions will alter the pH of the soil around the anode and cathode, respectively. The soil near the anode becomes more acidic, whereas the soil near the cathode becomes more basic. Furthermore, gas bubbles generated on the surface of the electrodes increase the resistance, thereby reducing the current and treatment efficiency.

During the tests in our work, a hissing sound appeared to be generated at the electrodes, and a strong smell from the emitted gas was observed. At the end of the tests, the anode removed from test A was observed to be severely corroded. The original mass of 117.19 g was reduced to 83.25 g after all the oxidized materials on the surface of the anode were removed, equating to a reduction of 33.94 g. Meanwhile, both corrosion and reduction of cathode were negligible, and a slight increase in the cathode mass from 139.24 g to 139.81 g was observed during the test A. In test B, corrosion was observed at the anode but was significantly less severe than in that test A. The mass was reduced from 118.61 g to 98.83 g for a total reduction of 19.78 g after the removal of all the oxidized material. No obvious difference in the cathode mass was observed before or after the test.

### 3.5 Current and power consumption

A constant 10V DC voltage was applied during the electroosmotic stage. The straight-line distance between the cathode and anode was 17.0 cm. The curve for the electrical current used with time in the test is plotted in Fig. 12. The currents in tests A and B both decreased with increases in the test time, and the drop in current in test B was more significant than that in test A.

The electrical energy consumption during electroosmosis, $E$, can be calculated using

$$E = \int \frac{V \cdot I \cdot t}{1\,000} \mathrm{d}t \quad (5)$$

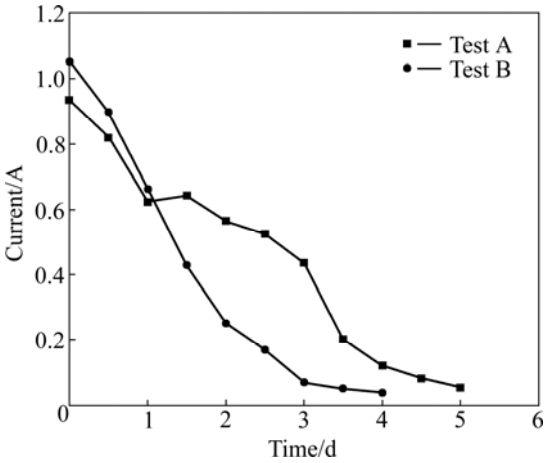


**Fig. 12** Current variation with time during electroosmosis with applied voltage of 10 V

where $V$ is voltage (V), $I$ is current (A), and $t$ is processing time (h). The energy consumption in test A was calculated to be 0.542 kWh, whereas the consumption in test B was 0.356 kWh. Considering the effect of the electroosmotic reinforcement region illustrated by the shadowed area of Fig. 3(a), and using a depth of 55 cm, the energy consumption per unit volume of soil was calculated to be 63.1 kWh/m$^3$ in test A and 41.4 kWh/m$^3$ in test B.

The vacuum used in this work was provided using a TW-4A single-stage rotary vacuum pump with a power of 0.37 kW. Considering that there was no effect after about 10 d vacuum pumping, the energy used effectively during VP for tests A and B was 88.8 kWh, respectively, and the energy consumption per unit volume of soil was 302 kWh/m$^3$.

### 3.6 Soil strength

The strength of the soil was measured after the test using an E-286 vane shear apparatus. The vane shear dimensions were 16 mm × 32 mm and could be used to measure the undrained shear strength. The locations of the test points are indicated in Fig. 7, and two measurements were recorded at two depths (25 cm and 45 cm) at each test point. The undrained shear strength is summarized in Table 3.

Compared to the initial soil, the strength of the reinforced soil was significantly greater. After VP treatment, the average undrained shear strengths at the VP sampling locations in test A were 83 kPa (at 25 cm depth) and 68 kPa (at 45 cm depth), whereas the average undrained shear strengths in test B were 81 kPa (at 25 cm depth) and 69 kPa (at 45 cm depth), respectively.

After VP treatment and electroosmosis, variations in the undrained shear strength were closely related to the combined effects of VP. Reinforcement was observed to be significantly improved using the VPCEO method instead of the EOAVP method.

In test A, the undrained shear strengths in the VPCEO region was significantly greater than that in the VP region, as observed in the strength profiles shown in Fig. 13(a). The average soil strengths in the VPCEO region were 137 kPa (at 25 cm depth) and 111 kPa (at 45 cm depth). Using sampling points 4, 5, and 6 in the VP region of test A as control points, the increased undrained shear strengths of VPCEO anode test point 9, the midpoint between electrodes (point 8), and the cathode test point 7 after electroosmosis are summarized in Table 3. Compared to test point 4 in the VP region, the undrained shear strengths at the anode increased by 86%

**Table 3** Summary of undrained shear strength after reinforcement

| Location | Sample No. | Test A | | Test B | |
|---|---|---|---|---|---|
| | | 25 cm | 45 cm | 25 cm | 45 cm |
| VP area/kPa | 1 | 76 | 58 | 80 | 63 |
| | 2 | 86 | 72 | 82 | 67 |
| | 3 | 81 | 68 | 79 | 69 |
| | 4 | 78 | 59 | 74 | 61 |
| | 5 | 82 | 71 | 81 | 79 |
| | 6 | 93 | 80 | 90 | 74 |
| VPCEO area (Test A) or EOAVP area (Test B)/kPa | 7[a] | 139 (46) | 114 (34) | 87 (−3) | 72 (−2) |
| | 8[b] | 128 (46) | 102 (31) | 94 (13) | 81 (2) |
| | 9[c] | 145 (67) | 117 (58) | 110 (36) | 91 (30) |
| VP area/kPa | 10 | 85 | 68 | 82 | 64 |
| | 11 | 90 | 73 | 87 | 67 |
| | 12 | 79 | 56 | 75 | 54 |

a: Data in bracket are increase of Cu on the basis of point 6; b: Data in bracket are increase of Cu on the basis of point 5. c: Data in bracket are increase of Cu on the basis of point 4.

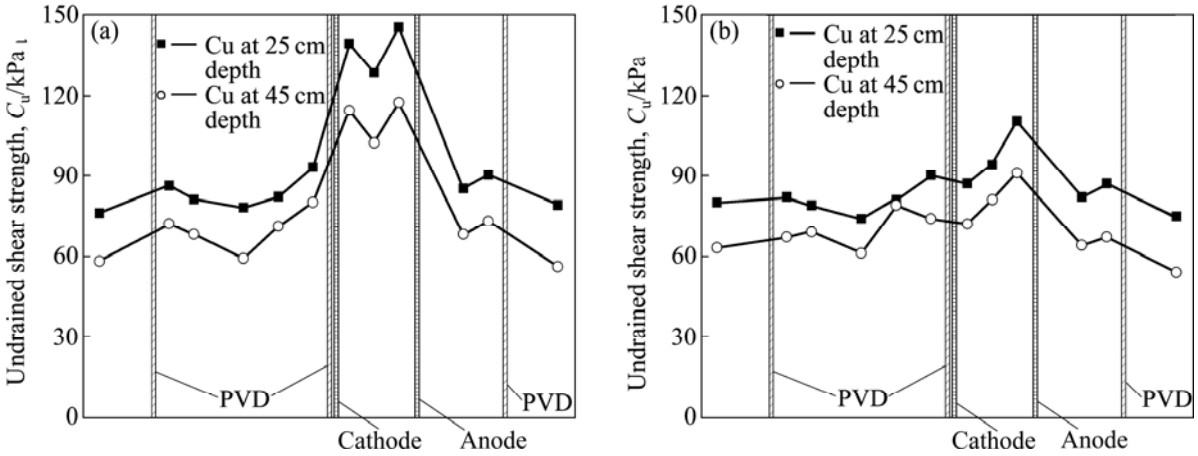


**Fig. 12** Distribution of undrained shear strength after reinforcement: (a) Test A; (b) Test B

(at 25 cm depth) and 98% (at 45 cm depth). Compared to test point 5, the increases in undrained shear strengths at the midpoint between electrodes were 56% (at 25 cm depth) and 44% (at 45 cm depth). With respect to test point 6, the undrained shear strengths at the cathode increased by 49% (at 25 cm depth) and 43% (at 45 cm depth).

In test B, the average undrained shear strengths of the sampling points in the EOAVP region were 97 kPa (at 25 cm depth) and 81 kPa (at 45 cm depth). The strengths at all test points are indicated in Fig. 13(b). As in test A above, using sampling points 4, 5 and 6 in the VP region as a reference, the increased undrained shear strengths of the EOAVP anode test point 9, the midpoint between electrodes (point 8), and the cathode test point 7 after electroosmosis are summarized in Table 3. A significant increase in the soil strength was observed at the anode. Compared to point 4 of the VP region, the increases in soil strength at the anode were 49% (at 25 cm depth) and 49% (at 45 cm depth). The midpoint between the two electrodes exhibited a slight increase in strength, and compared with point 5 of the VP region, the soil strengths at the midpoint of the two electrodes increased by 16% (at 25 cm depth) and 3% (at 45 cm depth). A slight decrease in soil strength was observed near the cathode, and compared to point 6 of the VP region, the soil strengths decreased by 3% (at 25 cm depth) and 3% (at 45 cm depth).

Based on the undrained shear strength results, soil reinforcement using the VP method yielded a significant increase in soil strength, which was further improved by the VPCEO method on a large scale. An increase in soil strength at the anode was observed using the EOAVP treatment; however, only a small increase was observed at the midpoint of the two electrodes, and a decrease in the strength was observed at the cathode.

### 3.7 Water content and void ratio

The water content and void ratios of the soil were measured after the tests. The sampling locations for the water content measurements are close to the vane shear test points 4, 6, 7, 8, and 9. Measurements were performed at three different depths (5, 25, and 45 cm). The void ratio sampling locations are close to the vane shear test points 4 and 9. Measurements were recorded at the depths of 5, 25, and 45 cm. The results are summarized in Table 4.

In test A, the initial water content was approximately 57%. After VP reinforcement, the water content ranged from 32.0%−38.1% within the reinforced region. In the VPCEO region, the water content at the top of the reinforced soil was less than that in the VP region. In the middle and lower depths of the reinforced soil, the water content at the anode and cathode were significantly less than those in the VP region. The water content at the anode had the lowest value.

In test B, the initial water content was approximately 57%. After VP reinforcement, the water content of the reinforced region was 33.2%−40.2%. In the EOAVP region, the water content at the anode was relatively small and was approximately 2% less than that of the same location in the VP region. The water content of regions near the cathode and the midpoint between the cathode and anode were similar to those in the VP region.

During the test, the average water content of the soil decreased significantly after the VP treatment. After electroosmosis, the water content decreased significantly in the VPCEO region of test A, whereas in test B, decreases in the water content were only observed in the areas near the anode of the EOAVP region, and the water content of all the other points did not change significantly.

**Table 4** Measured water content, void ratio and saturation degree after reinforcement

| Parameter | Depth/cm | Test A | | | | | Test B | | | | |
|---|---|---|---|---|---|---|---|---|---|---|---|
| | | 4 | 6 | 7 | 8 | 9 | 4 | 6 | 7 | 8 | 9 |
| $w$/% | 5 | 33.1 | 32.1 | 33 | 33.7 | 32.0 | 34.2 | 33.2 | 34.0 | 33.7 | 32.6 |
| | 25 | 37.6 | 35.3 | 33.2 | 35.4 | 33.2 | 37.9 | 36.2 | 36.3 | 36.6 | 34.3 |
| | 45 | 37.7 | 38.1 | 36.2 | 38.2 | 34.4 | 40.2 | 38.3 | 38.6 | 39.6 | 37.4 |
| Void ratio | 5 | 1.015 | — | — | — | 1.011 | 1.021 | — | — | — | 1.024 |
| | 25 | 1.090 | — | — | — | 1.084 | 1.103 | — | — | — | 1.101 |
| | 45 | 1.101 | — | — | — | 1.103 | 1.126 | — | — | — | 1.121 |
| $S_r$/% | 5 | 88 | — | — | — | 85 | 90 | — | — | — | 86 |
| | 25 | 93 | — | — | — | 83 | 93 | — | — | — | 84 |
| | 45 | 92 | — | — | — | 84 | 96 | — | — | — | 90 |

The initial void ratio of the soil was $e_0$=1.553, and after VP reinforcement, the void ratio of both tests decreased to 1.015−1.126. The void ratios in the VPCEO and EOAVP regions were similar to those in the VP region after reinforcement, thus indicating that no significant change of void ratio was induced by electroosmosis. Therefore, the saturation of the reinforced region was calculated, and as indicated in the table, the saturation of the VPCEO and EOAVP regions decreased after electroosmosis.

## 4 Discussion

### 4.1 Reinforcement effect of VP, VPCEO and EOAVP

The VP method can effectively promote the compression and settlement of soft soil, reduce the water content, and increase the strength of the soil. In tests A and B, the average settlements during the VP period were 62.6 and 65.8 mm, respectively, and the reinforced soil depth $H$ was 60 cm, with compression ratio of 1.0%−1.1%. The average water content of the reinforced soil decreased from 57.0% to 32.0%−40.2% with a reduction of 16.8%−25.0%. The undrained shear strength increased from 9 kPa to 81−83 kPa (the average value for the site at a depth of 25 cm after reinforcement), with an increase of 822%−889%.

The VPCEO method was performed by applying electroosmosis when the effect of VP diminished. When electroosmosis and VP were conducted together, the settlement of the soil was not apparent, with a settlement of 1.7 mm. The average water content was reduced by 0.8%−1.2%. The undrained shear strength increased significantly beyond that of the VP reinforcement method. At a depth of 25 cm, the average undrained strength increased from 84 kPa to 137 kPa, indicating an increase of 63.1%. At a depth of 45 cm, the average undrained shear strength increased from 70 kPa to 111 kPa, indicating an increase of 58.6%.

The EOAVP method was similar to the VPCEO method, with the exception that the vacuum was released before applying electroosmosis. During electroosmosis, the settlement of soil was not apparent, with a settlement of 1.2 mm. The average water content decreased 0.8%. The undrained shear strength exhibited a significant increase near the anode and a slight increase at the midpoint between the electrodes, whereas no increase was observed at the cathode.

The reinforcement effect of VPCEO was better than that of EOAVP significantly, mainly reflected in the increase of soil's undrained shear strength.

### 4.2 Soil strengthening mechanism of VPCEO

Based on the experimental results, the soil strength increased dramatically after treatment, which is partially due to the reinforcement afforded by VP. In addition, with the application of electroosmosis after VP, as observed in the VPCEO regions of test A and the EOAVP regions of test B, a further increase in strength was observed. During the electroosmotic stage, whether the electroosmosis was performed alone or in combination with VP, the improvement in settlement was minor. In test A, the settlement was 1.7 mm in the VPCEO region after electroosmosis, whereas for test B, it was 1.2 mm in the EOAVP region. The compression of soil skeleton induced by electroosmosis was very small, and virtually no apparent change was observed in the void ratio. However, a significant increase in the soil strength was observed in the VPCEO region in test A, similar to that observed around the anode in the EOAVP region of test B. The results show that the soil strength increased significantly, whereas the variations in both settlement and void ratio were small, which suggest that the mechanism of soil strengthening during electroosmosis in this work is attributed to electrochemical reactions.

As mentioned above, chemical reactions occur at both the anode and cathode during electroosmosis. The most common chemical reactions include the electrolysis of water and the redox reactions of the metal electrodes.

The electrolysis of water can reduce the water content surrounding the electrodes. In test A, the water content in the soil around both the anode and cathode exhibited an appreciable decrease. In contrast, the water content in the soil around the anode decreased in test B, although only a negligible decrease was observed near the cathode, which can be explained by the fact that with the current flowing from the anode to the cathode, the water accumulated near the cathode was not readily discharged.

In this work, the metal used at the anode was aluminum and that used at the cathode was copper. With the electroosmosis, Al oxidizes to become $Al^{3+}$, releases $O_2$, and produces $H^+$, whereas at the cathode, $H_2$ is released and $OH^-$ is produced. In the process of ion diffusion and migration, both $Al^{3+}$ and $H^+$ diffuse from the anode to the cathode, and $OH^-$ diffuses from the cathode to the anode. When $Al^{3+}$ ions collide with $OH^-$, the following reaction occurs:

$$3OH^- + Al^{3+} \rightarrow Al(OH)_3 \downarrow \quad (6)$$

An aluminum hydroxide colloid is produced that increases the strength of the soil. X-ray fluorescence (XRF) analysis was conducted on soil samples before and after the test, and the locations of the collected samples are close to the vane shear test points 4, 7, 8, and 9. At each location, three samples were collected for the same analysis. An ARL-9800XP+ XRF spectrometer was used in this work, and the element analysis was conducted according to the specifications of "The People's Republic of China's Nonferrous Metals Industry Standard YS/T 575.23—2009". The average element contents of the collected soils are presented in Table 5.

Because XRF analysis requires heat treatment of the samples prior to analysis, the aluminum hydroxide is converted to $Al_2O_3$, as demonstrated in the following reaction:

$$2Al(OH)_3 \xrightarrow{\text{Heating}} Al_2O_3 + 3H_2O \quad (7)$$

All other metal hydroxides also undergo a similar reaction; therefore, all of the element contents detected by XRF analysis were derived from oxide species. Compared to the original soil before treatment, the $Al_2O_3$ content increased within the VPCEO region. Increases of 2.2%, 1.5%, and 0.9% were recorded at the anode, the midpoint between electrodes, and the cathode, respectively. Within the EOAVP region, an increase in the $Al_2O_3$ content was also observed, although to a lesser extent when compared with the VPCEO region. The recorded increases were 1.1% at the anode, 0.6% at the midpoint between electrodes, and 0.1% at the cathode, which were negligible increases. In both tests, the variations in the $Al_2O_3$ contents agreed well with the variations of soil strength, thereby confirming that the soil strengthening resulted from the electrochemical reactions caused by electroosmosis.

### 4.3 Effect of VP on electroosmosis

The soil strengthening effect of electroosmosis was not uniform, and strength increases in the soil near the cathode were small. Based on the data obtained in this series of experiments, significant strength increases were only detected at the anode in the EOAVP regions, whereas a significant increase in soil strength was observed for the entire VPCEO region. The effect of VP during electroosmosis is apparent. Although VP is a purely physical-mechanical process, the provided vacuum can facilitate electroosmosis in various ways as follows:

**Table 5** Element contents of soil from XRF analysis (mass fraction, %)

| Element | Original sample | Test A | | | Test B | | |
|---|---|---|---|---|---|---|---|
| | | Anode | Midpoint | Cathode | Anode | Midpoint | Cathode |
| $SiO_2$ | 55.39 | 55.17 | 55.12 | 55.2 | 54.68 | 55.18 | 55.01 |
| $Al_2O_3$ | 18.14 | 18.54 | 18.42 | 18.3 | 18.34 | 18.25 | 18.16 |
| $Fe_2O_3$ | 6.03 | 6.07 | 6.04 | 6.08 | 5.97 | 5.97 | 5.95 |
| $K_2O$ | 3.43 | 3.47 | 3.47 | 3.52 | 3.45 | 3.47 | 3.47 |
| MgO | 2.81 | 2.88 | 2.96 | 2.97 | 2.82 | 2.94 | 2.95 |
| CaO | 2.71 | 2.73 | 2.9 | 2.86 | 2.95 | 2.65 | 2.81 |
| $Na_2O$ | 1.02 | 0.91 | 0.97 | 0.99 | 0.65 | 0.94 | 1.19 |
| $TiO_2$ | 0.8 | 0.76 | 0.77 | 0.78 | 0.78 | 0.78 | 0.78 |
| $SO_3$ | 0.42 | 0.52 | 0.28 | 0.37 | 0.58 | 0.52 | 0.41 |
| $P_2O_5$ | 0.15 | 0.13 | 0.14 | 0.13 | 0.14 | 0.14 | 0.11 |
| MnO | 0.15 | 0.16 | 0.16 | 0.17 | 0.17 | 0.15 | 0.16 |
| Cl | 0.25 | 0.24 | 0.04 | 0.06 | 0.32 | 0.25 | 0.05 |
| Loss on ignition | 8.53 | 8.29 | 8.42 | 8.44 | 9.00 | 8.68 | 8.81 |

1) In the process of electroosmosis, the generated $H_2$ and $O_2$ gases at the electrodes are difficult to remove, and they thus remain at the surface of the electrode, thereby increasing the overall electrical resistance. This phenomenon reduces the efficiency of electroosmosis and even halts the process altogether. When used in conjunction with VP, the gases generated during electroosmosis can be pumped out more readily, thus reducing the resistance surface area of the electrodes and increasing the electroosmotic efficiency.

2) When electroosmosis is conducted in the absence of a vacuum, water flow that has migrated to the cathode through electroosmotic flow cannot be discharged readily, thus affecting the soil strengthening efficiency. As discussed previously, the soil strength near the cathode of the EOAVP region decreases. Under vacuum, the cathode and the PVD are in contact; thus, water that has migrated to the cathode can be removed more readily and no longer negatively affects the soil-strengthening mechanism.

3) The soil strengthening effect of electroosmosis is not uniform, and as demonstrated at the anode and cathode in the EOAVP region, the increase in soil strength varies greatly. Although the soil strengthening effect is greater near the PVD relative to positions between the PVDs using VP alone. If electroosmosis is conducted in conjunction with VP, a much more uniform soil strengthening effect will result. This strengthening effect results from the combination of the cathode and the PVD, being brought near each other by the vacuum, and the anode, being placed between the PVDs.

4) In the process of electroosmosis alone, small cracks can be observed in the soil around the anode, which increase the electrical resistance, resulting in greater electrical power consumption. In the presence of a vacuum, pressure is exerted uniformly in all directions and thus forces the soil to contract, thereby reducing the formation of cracks.

### 4.4 Applicability and economic consideration of VPCEO

The use of electroosmosis in geotechnical engineering was considered to be uneconomical, which was the main reason for its limited use. A large variation in the energy consumption during electroosmosis has been reported in the literature. The energy consumption of electroosmosis is reported in a range of 0.7−230 $kW·h/m^3$ [10]. In this work, the energy consumption was 302 $kW·h/m^3$ during the VP phase and was 63.1 $kW·h/m^3$ during the electroosmosis period. The total power consumption in the electroosmotic phase was 21% of that used in the VP phase. In engineering practice, the total energy consumption of vacuum preloading is approximately 24.3−31.5 $kW·h/m^2$ [19]. If the soil depth was considered, which is about 20 m, the energy consumption will be only 1.22−1.58 $kWh/m^3$. The energy consumption measured in laboratory tests can differ greatly when compared to practical applications, and thus, estimating the economic value of VPCEO in this work remains a challenge. However, it is affirmatory that the energy consumption of electroosmosis in VPCEO is considerably less than that of normal electroosmosis due to most of the pore water was discharged by vacuum preloading.

The results of this work demonstrated that the VPCEO treatment is applicable to areas such as silt and sludge sites that require a high bearing capacity. However, if the purpose of soft-soil treatment engineering is to reduce settlement, such as in applications used for highways, the VPCEO method is not suitable because the settlement during electroosmosis was quiet small.

## 5 Conclusions

1) VPCEO is suitable for strengthening silt and soil fields that require a high bearing capacity. However, VPCEO is not an ideal method for applications intended to reduce settlement. VPCEO treatment provides a further increase in soil strength compared to VP treatment alone, along with a further reduction in water content within the soil. However, a reduction in the settlement of the soil is not apparent. The average undrained shear strength at a depth of 25 cm increases from 84 kPa to 137 kPa, with an increase of 64%, whereas the strength increases from 70 kPa to 111 kPa at a depth of 45 cm, with an increase of 59%. During VPCEO treatment, the settlement is negligible within the VPCEO region, with a value of 1.7 mm. And the reinforcement effect of VPCEO is significantly better than that of EOAVP, this mainly is reflected in the increase of soil's undrained shear strength. In EOAVP, only slightly increase of the soil strength is observed between the two electrodes, and even with a small decrease in soil strength around the cathode.

2) Electroosmosis is conducted in the late stage of VP, and the water drainage was apparent, but the soil consolidation is not apparent. Within the VPCEO region, the increase in the soil strength is caused by electrochemical reactions during electroosmosis. These reactions result in a decrease in the water content near each electrode and the release of $Al^{3+}$ ions through the oxidation of the Al anode, which then react with $OH^-$ ions to form an $Al(OH)_3$ colloidal precipitate that effectively increases the soil strength. XRF analysis reveals that compared to the soil before treatment, the concentrations of $Al_2O_3$ in the VPCEO region increase by 2.2%, 1.5%, and 0.9% at the anode, the midpoint

between the electrodes, and the cathode, respectively. In the EOAVP region, the increases in $Al_2O_3$ contents are observed to be 1.1% at the anode, 0.6% at the midpoint between the two electrodes, and 0.1% at the cathode, which are less than the corresponding values for the VPCEO region. The increase in $Al_2O_3$ content is in agreement with the change in soil strength.

3) The application of a vacuum enhances the effectiveness of electroosmosis. The $H_2$ and $O_2$ generated at the surface of the electrodes can be removed by the vacuum, which reduces the resistance of the electrode surface and thus reduces the energy consumption, thereby increasing the electroosmotic efficiency. With VPCEO, the cathode is placed adjacent to the PVDs and the anode is placed between the PVDs; the combination of the two methods will result in a more uniform reinforcement effect. This arrangement of placing the cathode adjacent to the PVD increases the drainage of water away from the cathode, thus removing the negative effects of water accumulation on the soil strength. The vacuum can cause the soil to contract and thus reduce the formation of cracks, which decreases the energy consumption of electroosmosis.

4) The power consumption of the laboratory tests during the VP phase is 302 kWh/m$^3$, whereas the power consumption during the VPCEO phase is 63.1 kWh/m$^3$. Because the differences in energy consumption between laboratory tests and field applications are large, it is difficult to directly calculate the economic value of the VPCEO. Because most of the pore water is discharged by vacuum preloading, it is undoubted that the energy consumption of electroosmosis in VPCEO is considerably less than that of normal electroosmosis.

## Acknowledgements

Thanks are given to Prof. GAO Yu-feng and Associate Prof. LIU Jun for help to English improvement and submission suggestion of this work, who both come from the Geotechnical Research Institute of Hohai University, China.

## References

[1] LIU Ci-gui. Report on the manage of oceanic exploit in 2007−2011 [R]. China Oceanic Information Network, 2011−2012.

[2] KJELLMAN W. Consolidation of clayey soils by atmospheric pressure [C]// Proceedings of a Conference on Soil Stabilization. Boston: Massachusetts Institute of Technology, 1952: 258−263.

[3] COGNON J M, JURAN I, THEVANAYAGAM S. Vacuum consolidation technology-Principles and field experience [R]. Proc Conf on Vertical and Horizontal Deformations of Foundations and Embankments Deformations. College Station, 1994: 1237− 1248.

[4] INDRARATNA B, SATHANANTHAN I, RUJIKIATKAMJORN C, BALASUDRAMANIAM A S. Analytical and numerical modeling of soft soil stabilized by PVD incorporating vacuum preloading [J]. International Journal of Geomechanics, 2005, 5(2): 114−124.

[5] SHANG J Q, TANG M, MIAO Z. Vacuum preloading consolidation of reclaimed land: A case study [J]. Canadian Geotechnical Journal, 1998, 35(3): 740−749.

[6] INDRARATNA B, RUJIKIATKAMJORN C, AMERATUNGA J, BOYLE P. Performance and prediction of vacuum combined surcharge consolidation at port of Brisbane [J]. Journal of Geotechnical and Geoenvironmental Engineering, 2011, 137(11): 1009−1018.

[7] CHAI J C, CARTER J P, HAYASHI S. Vacuum consolidation and its combination with embankment loading [J]. Canadian Geotechnical Journal, 2006, 43(10): 985−996.

[8] CASAGRANDE L. Electro-osmotic stabilization of soils [J]. Journal of the Boston Society of Civil Engineers, 1952, 39(1): 51−83.

[9] LAURSEN S. Laboratory investigation of electroosmosis in bentonites and natural clays [J]. Canadian Geotechnical Journal, 1997, 34(5): 664−671.

[10] KANIRAJ S R, HUONG H L, YEE J H S. Electro-osmotic consolidation studies on peat and clayey silt using electric vertical drain [J]. Geotechnical and Geological Engineering, 2011, 29(3): 277−295.

[11] BURNOTTE F, LEFEBVRE G, GRONDIN G. A case record of electroosmotic consolidation of soft clay with improved soil-electrode contact [J]. Canadian Geotechnical Journal, 2004, 41(6): 1038−1053.

[12] HU Li-ming, WU Wei-ling, WU Hui. Theoretical analysis and numerical simulation of electroosmosis consolidation for soft clay [J]. Rock and Soil Mechanics, 2010, 31(12): 2977−3983.

[13] LO K Y, HO K S, INCULET I I. Field test of electroosmotic strengthening of soft sensitive clays [J]. Canadian Geotechnical Journal, 1991, 28(1): 74−83.

[14] CHEW S H, KARUNARATNE G P, KUMA V M, LIM L H, TOH M L, HEE A M. A field trial for soft clay consolidation using electric vertical drains [J]. Geotextiles and Geomembranes, 2004, 22(1): 17−35.

[15] GOPALAKRISHNAM S, MUJUMDA A S, WEBER M E, PIEKONEN M. Electrokinetically enhanced vacuum dewatering of mineral slurries [J]. Filtration and Separation, 1996, 33(10): 929−932.

[16] GAO Zhi-yi, ZHANG Mei-yan, ZHANG Jian. Laboratory model test of vacuum preloading in combination with electro-osmotic consolidation [J]. China Harbour Engineering, 2000, 19(5): 58−61.

[17] FANG Ying-guang, XU Min, ZHU Zhong-wei. Experimental investigation into draining consolidation behavior of soda residue soil under vacuum preloading-electro-osmosis [J]. Journal of South China University of Technology: Natural Science Edition, 2006, 34(11): 70−75.

[18] ALSHAWABKEH A N, GALE R J, OZSU-ACAR E, BRICKA R M. Optimization of 2-D electrode configuration for electrokinetic remediation [J]. Journal of Soil Contamination, 1999, 8(6): 617−635.

[19] SHANG J Q. Electroosmosis-enhanced preloading consolidation via vertical drains [J]. Canadian Geotechnical Journal, 1998, 35(3): 491−499.

**(Edited by HE Yun-bin)**